Clays and Clay Minerals, Vol. 53, No. 6, 613–621, 2005.

PREPARATION AND CHARACTERIZATION OF Fe-PILCS. INFLUENCE OF THE SYNTHESIS PARAMETERS

José Luis Valverde[1], Amaya Romero[1,*], Rubí Romero[2], Prado Belén García[1], María Luz Sánchez[1] and Isaac Asencio[1]

[1] Facultad de Ciencias Químicas/Escuela Técnica Agrícola, Departamento de Ingeniería Química, Universidad de Castilla-La Mancha, Campus Universitario s/n, 13071 Ciudad Real, Spain

[2] Facultad de Química, Universidad Autónoma del Estado de México, Paseo Colón esq. Paseo Tollocan s/n, Toluca, Estado de México, México

Abstract—Iron-pillared clays (Fe-PILCs) were synthesized from hydrolyzed $FeCl_3$ solutions added to NaOH solutions using different synthesis conditions. X-ray diffraction, N_2 adsorption-desorption, chemical analysis, thermogravimetric analysis, differential thermal analysis, temperature-programmed desorption of ammonia and temperature-programmed reduction were used to characterize the resulting Fe-pillared clays (Fe-PILCs). A higher degree of pillaring was obtained when the Fe content was adjusted to 60 mmoles of Fe/g of clay. It was observed that higher values of this ratio led to worse acidity and textural characteristics, a consequence of the probable formation of Fe oxides that could not only deposit on the surface but also block the pores formed during the pillaring process. Likewise, it was found that the amount of Fe that can be introduced depended on the OH/Fe ratios. Total surface and micropore area decreased and Fe content increased with increasing pillaring solution concentrations. Finally, all pillared samples prepared here were thermally stable at temperatures up to 400ºC.

Key Words—Acidity, Basal Spacing, Iron, Pillared Clay, Surface Area, Synthesis.

INTRODUCTION

Pillared clays are two-dimensional zeolite-like materials prepared by exchanging charge-compensating cations between the clay layers with large inorganic metal hydroxycations which are oligomeric and are formed by hydrolysis of metal oxides or salts (Baes and Mesmer, 1976). After calcination, the metal hydroxycations are decomposed into oxide pillars that keep the clay layers apart and create interlayer interpillar spaces, thereby exposing the internal surface of the clay layers. The polyoxymetal cations apparently aggregate to form cationic oligomers in solution. The size of these oligomers appears to control the size of the pore openings in the pillared clay. In principle, any metal oxide or salt that forms polynuclear species upon hydrolysis can be inserted as a pillar (Baes and Mesmer, 1976; Burch, 1988; Clearfield, 1994; Sprung *et al*., 1990; Shabatai *et al*., 1984).

Intercalated clays are usually natural smectite clays. Smectite clays are readily pillared because of their low charge density and their swelling ability (Cañizares *et al*., 1999). Properties such as acidity, surface area, pore-size distribution and hydrothermal stability depend on the method of synthesis as well as on the nature of the host clay.

A wide variety of factors can influence the intercalation/pillaring process. This variety makes it difficult to compare the results obtained by different authors and good reproducibility is hard to achieve. The factors that influence the process include the nature of the host clay used as the parent material, the nature of the metallic cation, the hydrolysis conditions (concentration, time and ageing), the reaction time, the synthesis temperature and, finally, the washing, drying and calcination processes.

Despite the large number of papers concerning pillared clays (PILCs) with pillars of Al or Zr, only a limited number of papers dealing with Fe-PILC synthesis, uses and catalytic applications have been published to date (Kloprogge, 1998).

The preparation of Fe-PILC was first reported by Tzou and Pinnavaia (1983) who prepared pillared clays starting from pillaring solutions of $FeCl_3$, $Fe(NO_3)_3$, $Fe(ClO_4)_3$ and $Fe_2(SO_4)_3$. Further papers recognized Fe-pillared clays as interesting catalysts for the Fischer-Tropsch process (Burch *et al*., 1987; Kloprogge, 1998), selective catalytic reduction of NO_x by NH_3 or hydrocarbons (Yang *et al*., 1992), CO hydrogenation (Zurita *et al*., 1996), Friedel-Crafts reactions (Choudary *et al*., 1997; Duxiao *et al*., 2001), ring opening of oxiranes (Kantam *et al*., 1999), cyclohexane oxidation in gas phase (Carvalho, 2002), oxidation of phenol (Guelou, 2003), and ethylbenzene dehydrogenation (Huerta *et al*., 2003). These catalysts showed a pronounced shape selectivy that has been attributed to steric hindrance originating in the micropores of the material (Kloprogge, 1998).

The aim of the work described here was to synthesize and characterize Fe-PILCs from bentonite and a pillaring

* E-mail address of corresponding author:
amaya.romero@uclm.es
DOI: 10.1346/CCMN.2005.0530607

solution containing $FeCl_3 \cdot 6H_2O$. The influence of the main synthesis conditions (*i.e.* concentration of the pillaring solution, OH/Fe molar ratio, amount of Fe and clay suspension concentration) on the properties of the resulting clays was investigated. The ultimate goal was to obtain a material with the best possible physical properties.

EXPERIMENTAL

Fe-PILC preparation

The starting clay used was a purified-grade bentonite supplied by Fisher Scientific, with a cation exchange capacity of 94 meq/100 g of clay and the following chemical composition (wt.%): SiO_2, 52.22; Al_2O_3, 16.81; Fe_2O_3, 3.84; Na_2O, 1.26; MgO, 0.88; CaO, 0.74; K_2O, 0.80 (Cañizares *et al.*, 1999; Valverde *et al.*, 2003). Particle sizes <2 μm were used in the pillaring process.

A typical Fe-PILC synthesis procedure was as follows: $FeCl_3 \cdot 6H_2O$ was added to NaOH solutions to obtain the required OH/Fe molar ratio. In order to avoid precipitation of Fe species, the pH was kept constant at 1.7. The resulting solution was aged for 4 h with stirring at room temperature. It was observed that ageing times of <12 h did not have any practical influence on the physical properties of the pillared materials. The pillaring solution was then slowly added to a suspension of bentonite in deionized water. The mixture was stirred and allowed to react. Finally, the solid was washed by vacuum filtration with deionized water until it was chloride free (conductivity <6 μS/cm). The aim of this stage was to remove excess chloride ions which could prevent the diffusion of polyoxocations within the interlayer space (Palinko *et al.*, 1996). The solid was air dried and the resulting product was calcined for 2 h at different temperatures. The conditions used in the preparation of all the materials described are shown in Table 1. Notations for all of these samples are also given in Table 1.

CHARACTERIZATION TECHNIQUES

The X-ray diffraction (XRD) patterns in the range 3−20°2θ were obtained using a Philips PW 1710 diffractometer with Ni-filtered CuKα radiation at a scan speed of 0.02°2θ min^{-1}. In order to maximize the 001 reflection intensities, oriented clay-aggregate specimens were prepared by drying clay suspensions on glass slides. All the XRD patterns were background corrected. The XRD pattern of the parent clay exhibits a peak at ~9°, which is commonly assigned to the basal 001 reflection (d_{001}). In pillared clays, the d_{001} peak was found to shift towards the lower 2θ region, which is a clear indication of the enlargement of the basal spacing of the clay. The thermal stability of samples was investigated by exposing the materials in air to temperatures in the range 110−500°C for 2 h.

Surface area and pore-size distribution were determined using N_2 as the sorbate at 77 K in a static volumetric apparatus (Micromeritics ASAP 2010 sorptometer). Pillared clays were outgassed prior to use at 180°C for 16 h under a vacuum of 6.6×10^{-9} bar. Specific total surface areas were calculated using the BET equation, whereas specific total pore volumes were evaluated from N_2 uptake at $(P/P_0) = 0.99$. The Horvath-Kawazoe (H-K) method was used to determine the micropore surface area and volume (Horvath and Kawazoe, 1983). The Barrett, Joyner and Halenda (BJH) method was used to determine the mesopore-

Table 1. Experimental conditions used in the preparation of Fe-PILCs.

Set of experiments	Sample designation	mmol Fe/g clay	OH/Fe ratio	Suspension clay concentration (wt.%)	Pillaring solution concentration (M)	Ageing time (h)
	Fe-PILC1	40	2.0	0.10	0.2	4
1	Fe-PILC2	60	2.0	0.10	0.2	4
	Fe-PILC3	70	2.0	0.10	0.2	4
	Fe-PILC4	60	1.5	0.10	0.2	4
2	Fe-PILC2	60	2.0	0.10	0.2	4
	Fe-PILC5	60	2.5	0.10	0.2	4
	Fe-PILC2	60	2.0	0.10	0.2	4
3	Fe-PILC6	60	2.0	0.85	0.2	4
	Fe-PILC7	60	2.0	1.15	0.2	4
	Fe-PILC2	60	2.0	0.10	0.2	4
4	Fe-PILC8	60	2.0	0.10	0.5	4
	Fe-PILC9	60	2.0	0.10	1.0	4
	Fe-PILC6	60	2.0	0.85	0.2	4
5	Fe-PILC10	60	2.0	0.85	0.5	4
	Fe-PILC11	60	2.0	0.85	1.0	4

https://doi.org/10.1346/CCMN.2005.0530607 Published online by Cambridge University Press

size distribution (Barrett *et al.*, 1951). Surface area measurements have an error of ±3%.

Thermogravimetric analyses (TGA) were performed on 10 mg samples using a Perkin Elmer TGA 7 thermobalance under a helium flow (50 mL min^{-1}) with a heating rate of 15ºC min^{-1} from room temperature up to 900ºC.

The total acid site densities of the catalysts were measured by temperature-programmed desorption of ammonia (TPDA) using a Micromeritics TPD/TPR 2900 analyzer with a thermal conductivity detector (TCD). The samples were housed in a tubular quartz reactor and pretreated in a flow of helium while heating at 15ºC/min up to the calcination temperature of the sample. After a period of 60 min at this temperature, the samples were cooled to 180ºC and saturated for 15 min in a stream of ammonia. The sample was then allowed to equilibrate in a helium flow at 180ºC for 1 h. The ammonia was then desorbed using a linear heating rate of 15ºC/min up to 400ºC. Temperature and detector signals were recorded simultaneously. The unique area under the curve was integrated in each case to determine the total acidity of the sample.

Temperature programmed reduction (TPR) measurements were carried out with the same apparatus described above. After loading, the sample was outgassed by heating at 15ºC/min in an argon flow up to the calcination temperature and kept constant at this temperature for 30 min. The sample was then cooled to room temperature and stabilized under an argon/hydrogen flow (⩾99.9990% purity, 83/17 volumetric ratio). The temperature and detector signals were then continuously recorded while heating at 15ºC/min up to 500ºC. The liquids formed during the reduction process were retained by a cooling trap placed between the sample and the detector. The TPR profiles are reproducible, with standard deviations for the temperature of the peak maxima being ±2%.

The Fe content (wt.%) of the prepared materials was determined by atomic absorption measurements using a SPECTRAA 220 FS analyzer with simple beam and background correction and an error of ±1%. For the digestion of the samples, the minimum amount of hydrofluoric acid (45%) was used. After digestion (3 h), samples were diluted with demi-water to the range of measurement. It was not necessary to neutralize the HF because the sensitive parts of the AAS equipment were made of a resistant material. The standards were prepared by dilution from commercial solutions for spectrophotometry (PANREAC, 1±0.002 g/l). It is important to note that in all the samples the concentration of the Fe complex was greater than the CEC of the original clay.

RESULTS AND DISCUSSION

Influence of Fe content (Set 1)

The basal spacings corresponding to both the parent clay and those of the all Fe-PILCs calcined at different temperatures are shown in Table 2. Set 1 was carried out using pillaring solutions with 40, 60 and 70 mmoles of Fe/g of clay. A peak corresponding to the 001 reflection appeared at smaller angles (~4º2θ) than in the corresponding parent clay (~9º2θ) in each case. This fact clearly indicates an enlargement of the basal spacing of the clay as a consequence of the pillaring process. In these samples a broader peak in the range ~7–8º2θ (sometimes not clearly defined) was observed, which can be attributed to two overlapped peaks: the 002 reflection of the pillared clay and the 001 reflection

Table 2. Basal spacing (Å) of Fe-PILCs calcined at different temperatures.

Set of experiments	Sample	110ºC		200ºC		300ºC		400ºC		500ºC	
		1st peak	2nd peak	1st peak	2nd peak	1st peak	2nd peak	1st peak	2nd peak	1st peak	2nd peak
	Original clay	–	13.4	–	9.9	–	9.8	–	9.7	–	9.7
1	Fe-PILC1	n.c.d.*	12.7	n.c.d.	12.6	20.7	12.3	20.6	11.7	15.2	10.5
	Fe-PILC2	n.c.d.	13.1	22.2	12.8	27.8	11.9	25.1	12.4	15.8	12.1
	Fe-PILC3	n.c.d.	13.7	n.c.d.	12.1	21.1	11.4	–	10.3	–	9.7
2	Fe-PILC4	n.c.d.	13.0	n.c.d.	11.8	26.6	10.7	–	10.1	–	9.9
	Fe-PILC5	n.c.d.	12.3	25.4	12.2	25.9	13.3	23.9	11.5	–	9.6
3	Fe-PILC6	n.c.d.	12.2	22.1	12.1	25.5	10.6	22.5	10.3	–	9.9
	Fe-PILC7	–	14.0	–	10.1	–	10.0	–	9.8	–	9.7
4	Fe-PILC8	n.c.d.	13.9	22.1	11.3	26.3	11.7	24.5	12.2	–	12.0
	Fe-PILC9	n.c.d.	13.8	24.5	12.2	25.6	11.8	23.8	11.3	–	9.9
5	Fe-PILC10	n.c.d	12.3	n.c.d	10.9	23.1	10.3	23.0	10.2	–	9.8
	Fe-PILC11	n.c.d	13.0	n.c.d	13.5	20.5	10.1	–	9.5	–	9.4

1st peak: located at ~4º2θ
2nd peak: located at ~6–8º2θ (except for the original clay, which is located at 9º2θ)
*n.c.d. (not clearly defined)

https://doi.org/10.1346/CCMN.2005.0530607 Published online by Cambridge University Press

corresponding to the intercalation of a proportion of monomeric species of small size, similar to those reported by Valverde *et al.* (2002) for Ti-PILCs, thus leading to smaller openings of the clay layers (Cheng and Yang, 1995).

The interlayer spacing in Na-montmorillonite, originally occupied by hydrated Na^+ cations, is ~3.5 Å. After calcination, the clay structure collapses (d_{001} decreased to 9.7 Å) and the interlayer region becomes inaccessible to the N_2 molecules. Large and hydrated Fe polyoxocations introduced into the interlayer spaces of the clay push the sheets apart by ~15 Å (25 Å corresponding to d_{001}, *e.g.* Fe-PILC2 calcined at 400ºC, 9.6 Å corresponding to the thickness of the layers). Calcination of the Fe-pillared clays leads to the dehydration and dehydroxylation of Fe polycations and gives rise to the formation of polymeric Fe_2O_3 species which permanently link adjacent layers. The distance between the sheets of these pillared clays hardly decreases and the structure of the minerals still remains open up to 400ºC.

The N_2 adsorption/desorption isotherms for the samples Fe-PILC1, Fe-PILC2 and Fe-PILC3 calcined at 300ºC are shown in Figure 1. The isotherm shapes correspond to composite type I and type IV isotherms (Yamanaka *et al.*, 1987; Mishra *et al.*, 1996). The plot of the isotherms for Fe-PILCs at low relative pressure values (below 0.03) would correspond to type I according to the Brunauer, Deming, Derning and Teller (BDDT) classification (Sing *et al.*, 1985). This isotherm type is characteristic of microporous systems. Nevertheless, the plot of these isotherms at higher P/P_0 values would correspond to type IV, which is characteristic of materials that have relatively large pores (Cheng and Yang, 1995; Webb and Orr, 1997). The isotherm of the original clay also corresponds to type IV. It should be noted that all the isotherm data show a sharp jump upwards during the sorption stage at a relative pressure of ~0.75 and this may be due to data from two separate runs plotted together. The isotherm plateau allows us to deduce the internal superficial area by considering a monolayer adsorption of N_2 molecules. The presence of a hysteresis loop in all of the isotherms indicates some degree of mesoporosity. According to Hutson (1999), the mesoporosity is inherent in the clay itself, as shown by the hysteresis loop seen in the adsorption isotherm of the unpillared clay.

The degree of disorder in the clay flocs is the result of the attraction between negatively charged basal surfaces and positively charged crystal edges to form an internal "house of cards" structure (Van Olphen, 1963). The hysteresis loop corresponds to type H3 in the International Union of Pure and Applied Chemistry (IUPAC) classification and this is characteristic of material with slit-like pores. This finding is consistent with the structure expected for materials prepared by expanding a laminar structure (Mokaya and Jones, 1995).

The textural properties, acidity and Fe content of the samples prepared are shown in Table 3. Of the three samples, Fe-PILC2 yielded the greatest surface area. On the other hand, the acidity of the Fe-pillared clays may increase with the increase in both the Fe content forming the pillars (with a weak acid character) and the micropore area (leading to a higher NH_3 accessibility). As can be observed from the results in Table 3, Fe-PILC2 showed a slightly greater acidity value than the other two samples. These results clearly indicate that the opening of the clay sheet and the physical/chemical properties of the pillared clays depend on the quantity of the Fe complex inserted. Values of the ratio of mmoles of Fe/g of clay >60 (sample Fe-PILC2) led to a decrease in the surface area and acidity values, which could be due to a situation where some proportion of the Fe

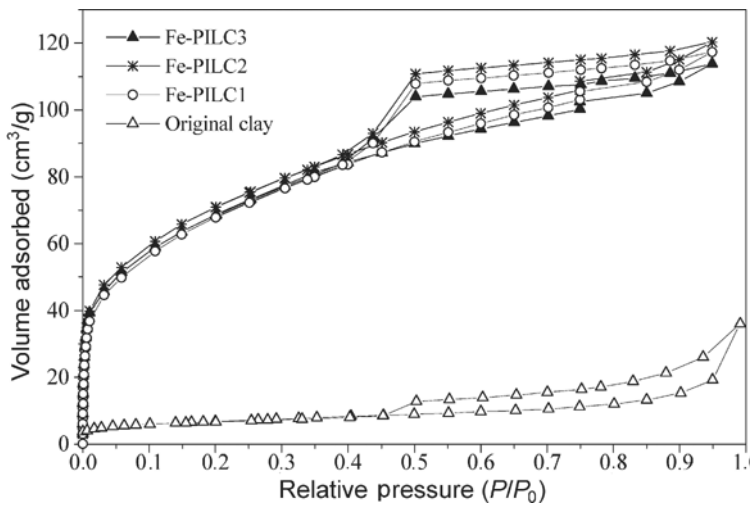

Figure 1. N_2-adsorption/desorption isotherms of the original clay and the samples prepared using 40, 60 and 70 mmoles of Fe/g clay (samples Fe-PILC1, Fe-PILC2 and Fe-PILC3)

https://doi.org/10.1346/CCMN.2005.0530607 Published online by Cambridge University Press

Table 3. Textural properties, acidity and Fe content of Fe-PILCs calcined at 300ºC.

Set of experiments	Sample	Surface area (m^2/g)	Micropore surface area (m^2/g) [1]	Pore volume (cm^3/g)	Micropore volume (cm^3/g)	Acidity (mmol NH_3/g)	Fe (wt.%)
	Original clay	36	15	0.060	0.003	0.132	2.7
1	Fe-PILC1	257	222 (86.5)	0.186	0.132	0.307	16.1
	Fe-PILC2	285	247 (86.7)	0.187	0.126	0.317	18.0
	Fe-PILC3	247	213 (86.3)	0.176	0.123	0.270	21.1
2	Fe-PILC4	218	164 (75.1)	0.174	0.084	0.311	26.4
	Fe-PILC5	230	198 (86.0)	0.161	0.111	0.295	16.0
3	Fe-PILC6	202	164 (81.3)	0.161	0.104	0.306	18.6
	Fe-PILC7	79	47 (60.0)	0.079	0.022	0.205	7.1
4	Fe-PILC8	270	232 (86.0)	0.185	0.123	0.301	20.5
	Fe-PILC9	266	232 (87.5)	0.185	0.133	0.307	24.3
5	Fe-PILC10	187	147 (78.9)	0.157	0.107	0.411	28.4
	Fe-PILC11	173	133 (76.9)	0.142	0.078	0.425	30.0

[1] Values in parentheses represent the percentage of micropores relative to the total area.

polyoxocations formed by association of the hydrated Fe cations are difficult to accommodate within the interlayer space. As a consequence, these species should be located on the external surface of the pillared clay, partially blocking its porous structure (Mishra *et al.*, 1996).

On the basis of the results obtained, sample Fe-PILC2 was selected as the reference for further studies.

The thermal stability of sample Fe-PILC2 was compared to that of the original clay (Figure 2). The TGA plot of the original clay showed a loss of 9 wt.% below 150ºC due to dehydration (loss of physically adsorbed water). Between 150 and 500ºC a very small weight loss (0.9 wt.%) was observed and this is attributed to the removal of interlayer water and the onset of dehydroxylation (Kloprogge *et al.*, 1994). Finally, dehydroxylation of the clay structure and its subsequent collapse caused a maximum weight loss of 4.5 wt.% between 500 and 800ºC. In the same way, Fe-PILCs showed three temperature intervals where the total weight loss was greater, but less pronounced, than that of the original clay. In the first interval (25–150ºC), the weight loss was due to the loss of physically adsorbed water and the dehydration of the chemical species that form the pillars. In the second interval (150–500ºC), the weight loss was attributed to dehydroxylation of both the clay structure and the Fe pillars, processes that are later accompanied by the structural collapse of the Fe pillars (Palinko *et al.*, 1996). The stability of the pillars is related to the dehydroxylation process that negatively affects the basal spacing (Molina, 2001) (see Table 2). At temperatures >500ºC an additional weight loss occurs and this is similar to that observed in the original clay (of ~4 wt.%).

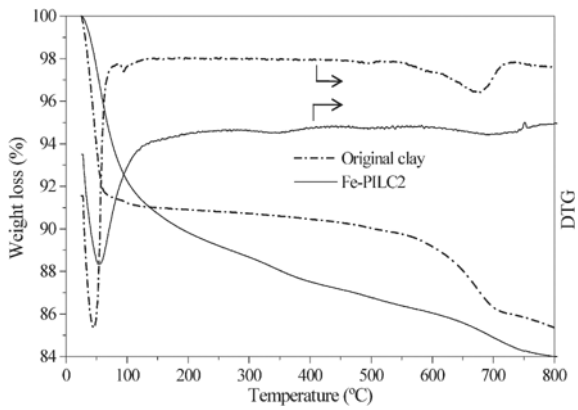

Figure 2. TGA and DTG curves of the original clay and sample Fe-PILC2.

Influence of the OH/Fe molar ratio (Set 2)

Different authors have demonstrated that the preparation of Fe-PILCs is affected by the OH/Fe molar ratio (Rightor *et al.*, 1991; Kloprogge, 1998). The amount of Fe that can be introduced inside the clay structure depends on the pH of the Fe-pillaring solution. A pH of 1.7 for this solution was used in this study. It has been demonstrated that pH values >1 but <1.8 promote the polymerization degree and polyoxocation exchange but pH values >1.8 cause precipitation of the products derived from the Fe salt hydrolysis (Sharpe, 1993).

The XRD patterns corresponding to these materials prepared using pillaring solutions with an OH/Fe molar ratio in the range 1.5–2.5 (Set 2) are shown in Figure 3a. A slightly greater intensity of the peak corresponding to the 001 reflection plane (~4º2θ) can be seen when an OH/Fe molar ratio of 2 was used (sample Fe-PILC2) and this is indicative of a more homogeneous distribution of pillars.

Fe-PILC corresponding to Set 2 showed a basal spacing (calculated from the peak at ~º2θ) in the range

https://doi.org/10.1346/CCMN.2005.0530607 Published online by Cambridge University Press

22–27 Å (Table 2). Small differences in the measurement should not be taken into consideration as the broadness of the 001 peak, which is characteristic of Fe-PILCs, causes an appreciable error in the measurement of the basal spacing. On the other hand, the second peak (located in the range ~6–8°2θ) corresponds to a basal spacing value in the range 10–13 Å. Similar results were observed in previous studies (Baes *et al.*, 1976; Rightor *et al.*, 1991). For instance, a basal spacing of 12 Å would correspond with an interlayer spacing of 2 Å, while a basal spacing of ~25 Å would correspond to an interlayer spacing of ~15 Å. As mentioned above, this last value is related to the presence between the clay layers of certain types of cations that result from Fe salt hydrolysis. According to Molina (2001), these cations would be spherical with sizes of ~15 Å. Reflections in the range 15–19°2θ can be considered as noise that is probably related to the delamination of the clay. The XRD patterns of Fe-PILC2 calcined at different temperatures are shown in Figure 3b. As can be observed, the peak corresponding to the 001 reflection became slightly more pronounced when the calcination temperature was increased to 300°C. In contrast, the peak appearing at ~6–8°2θ became less pronounced. These results indicate that a temperature increase (up to 300°C) generates a more homogeneous pillar distribution. Meaningful differences in the position of the reflection at ~4°2θ were not observed when the calcination temperature was increased; hence the calcination temperature did not affect the basal spacing, indicating the thermal stability of the materials up to 400°C. Furthermore, meaningful differences were not found in the textural characteristics of this sample calcined at different temperatures (surface area decreased by only 10 m^2/g when the calcination temperature was increased from 110°C to 400°C). At higher calcination temperatures (>400°C) the 001 peak intensity decreased and the peak in the range 6–8°2θ became broader and shifted to higher 2θ values. From these results we conclude that the maximum calcination temperature for the preparation of Fe-PILCs is 400°C.

Finally, textural analysis (Table 3) showed that the surface area increased when the OH/Fe ratio was increased, passing through a maximum and then decreasing again. On the other hand, acidity values remain approximately constant in the three prepared samples.

The sample obtained using an OH/Fe molar ratio of 2 (sample Fe-PILC2) showed the best physical properties and this was therefore used as the reference in the next experiments.

Effect of the clay suspension concentration (Set 3)

The conventional synthesis of pillared clays requires very dilute aqueous media. In this sense, few papers have reported the use of highly concentrated clay suspensions such as that described by Kaloidas *et al.* (1995) who prepared PILCs using a microwave oven. In order to decrease the amount of water needed in the synthesis (*i.e.* to increase the amount of pillared clay obtained in each synthesis), samples involving more concentrated clay suspensions were prepared.

The basal spacing values corresponding to the materials prepared using different clay suspension concentrations (namely 0.10, 0.85 and 1.15 wt.% – Set 3) are shown in Table 2. The d_{001} peak of the resulting pillared materials was found to shift towards lower 2θ values in samples pillared using clay suspension concentrations of 0.10 and 0.85 wt.% (samples Fe-PILC2 and Fe-PILC6). However, in the sample pillared using a clay suspension concentration of 1.15 wt.% (Fe-PILC7), only one peak at ~8.5°2θ was observed in the XRD pattern, corresponding

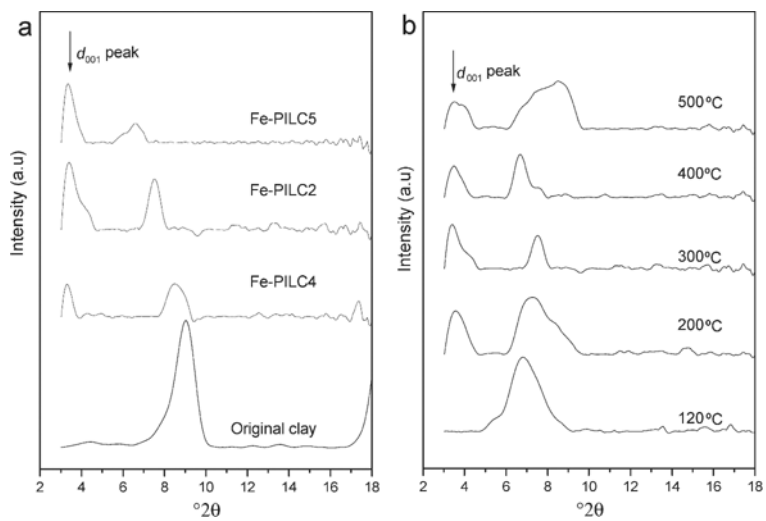

Figure 3. XRD patterns of (a) Fe-PILCs prepared using different OH/Fe molar ratios and calcined at 300°C and, (b) Fe-PILC2 calcined at different temperatures.

https://doi.org/10.1346/CCMN.2005.0530607 Published online by Cambridge University Press

to a basal spacing value similar to that of the original clay. This behavior clearly indicates that the ion-exchange process involving the initial charge-compensating cations of the clay and the Fe polyoxocations must depend on the clay suspension concentration. In this sample (Fe-PILC7), the pillaring process failed – a situation also supported by the smaller surface area value obtained. In samples pillared using clay suspension concentrations of 0.10 and 0.85 wt.%, a wider peak could be observed in the range ~7–8º2θ but this was less intense than that appearing at 4º2θ. This observation is related to the insertion of Fe polycations with a lower degree of polymerization (not shown).

The textural characteristics, acidity values and Fe content (wt.%) of the samples synthesized in Set 3 are given in Table 3. It can be observed that all of these parameters show the same trend with regard to the clay suspension concentration. As commented previously, acidity values, Fe content and micropore area are intimately related. This fact is supported by the results obtained. The best combination of micropore area and Fe content was obtained with Fe-PILC2 and, hence, a slightly higher acidity value was found for this sample.

As far as the calcination temperature is concerned, this factor markedly affects both the surface area (not shown) and basal spacing up to temperatures of ~400ºC due to dehydroxylation of the pillars. At temperatures up to 500ºC, pillars collapse and, as a consequence, dramatic decreases in the surface area and basal spacing values take place.

The TPR profiles of the samples prepared using clay suspension concentrations of 0.10 and 0.85 wt.% are shown in Figure 4 together with that of the oxide Fe_2O_3. This oxide material gives rise to an intense peak centered at 425ºC corresponding to the $Fe_2O_3 \rightarrow Fe_3O_4$ reduction process (Chen and Sachtler, 1998; Lee and Rhee, 1999). On the other hand, Fe-pillared clays present only one reduction peak centered at 350–370ºC and this corresponds to the $Fe^{3+} \rightarrow Fe^{2+}$ reduction process (Long *et al.*, 1999). It can be observed that this peak in sample Fe-PILC2 was shifted to higher temperatures, indicating that the Fe species in this case are more difficult to reduce. This fact is consistent with a major insertion of Fe species as pillars.

Samples Fe-PILC2 and Fe-PILC6 were selected as references for further studies. Sample Fe-PILC2 had the best textural characteristics and thermal stability; however, sample Fe-PILC6 was prepared with a higher-concentration clay suspension, which would lead to a cheaper production process.

Influence of the pillaring-solution concentration (Sets 4 and 5)

Basal spacing, textural properties, acidity and Fe content values of the Fe-PILCs prepared using Fe-pillaring solution concentrations of 0.2, 0.5 and 1 M and clay suspension concentrations of 0.1 (Set 4) and 0.85 wt.% (Set 5) are listed in Tables 2 and 3. The following trends were found: basal spacing values decrease marginally with increasing pillaring-solution concentrations; total surface and micropore area decreases with increasing pillaring-solution concentrations; the acidity was not affected by the pillaring-solution concentration in Set 4 but increased in Set 5, and Fe content increased with increasing pillaring-solution concentrations.

These results again seem to be related to the type of Fe species and their location in the clay. When the pillaring solution concentration increased, so did the amount of Fe located in the clay. However, not all of the Fe species were present in the pillars, as can be deduced from the similar acidity values observed for all the samples in Set 4. Excess Fe must be located outside the interlayer space. After calcination, this excess would give rise to Fe oxide particles, which could block the pore system of the clay and contribute to the decrease in the micropore surface area. Similar acidity values were obtained in all three samples and this is in agreement with the other results. Results obtained with pillared samples prepared in Set 5 were similar to those for samples in Set 4. The only difference between these two sets is that the increase in the Fe content was more prominent in Set 4 and, for this reason, the acidity values increased with increasing pillaring solution concentration.

However, the pillared sample obtained with the lowest concentration of the pillaring solution (Fe-PILC2) showed the highest values of surface area and micropore volume. These characteristics are related to the nature of the Fe species formed during the pillaring process.

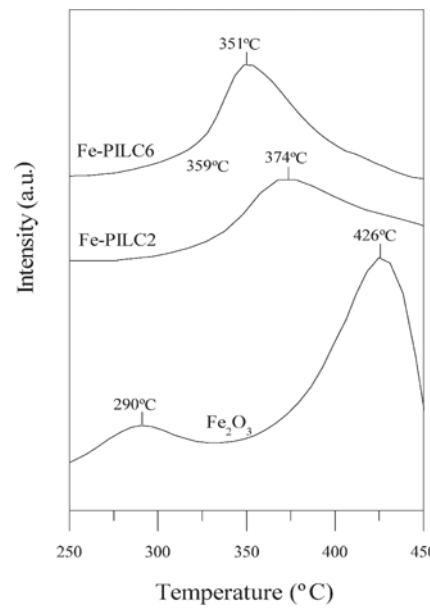

Figure 4. TPR profiles for Fe_2O_3 and samples Fe-PILC2 and Fe-PILC6 calcined at 400ºC.

https://doi.org/10.1346/CCMN.2005.0530607 Published online by Cambridge University Press

In conclusion, the pillared sample obtained from the pillaring solution with the lowest concentration (Fe-PILC2) showed the highest values of surface area and micropore volume – characteristics that are related to the nature of Fe species formed during the pillaring process.

CONCLUSIONS

Iron-pillared clays (Fe-PILCs) were synthesized from hydrolyzed $FeCl_3$ solutions added to NaOH solutions using different synthesis conditions. A greater degree of pillaring was obtained when the Fe content was adjusted to 60 mmoles of Fe/g of clay. It was found that acidity values decreased with increasing Fe contents – a consequence of the probable formation of Fe oxides that could not only be deposited on the surface, but also block the pores formed during the pillaring process. The amount of Fe that can be introduced inside the clay structure depended on the OH/Fe molar ratio: the best results were achieved when this ratio was 2.

The ion-exchange process involving the initial charge-compensating cations of the clay and the Fe polyoxocations was found to depend on the clay suspension concentration. The best combination of both micropore area and Fe content was obtained with the sample prepared from the lowest clay-suspension concentration. Total surface and micropore area decreased and Fe content increased with increasing pillaring solution concentrations.

Finally, the pillared samples prepared here were thermally stable up to temperatures of 400ºC.

ACKNOWLEDGMENTS

Financial support from the Ministerio de Ciencia y Tecnología (CICYT) of Spain (Projects PPQ2001-1195-C02-01 and CTQ2004-07350-C02-01) is gratefully acknowledged.

REFERENCES

Baes, C.F. and Mesmer, R.E. (1976) *The Hydrolysis of Cations*. Wiley, New York.

Barrett, E.P., Joyner, L.G. and Halenda, P.P. (1951) The determination of pore volume and area distributions in porous substances. I. Computations from nitrogen isotherms. *Journal of the American Chemical Society*, **73**, 373–380.

Burch, R. (1988) Introduction. *Catalysis Today*, **2**, 185–186.

Burch, R. and Warburton, C.I. (1987) Pillared clays as demetalization catalysts. *Applied Catalysis*, **33**, 395–404.

Cañizares, P., Valverde, J.L., Kou, M.R.S. and Molina, C.B. (1999) Synthesis and characterization of PILCs with single and mixed oxide pillars prepared from two different bentonites. A comparative study. *Microporous and Mesoporous Materials*, **29**, 267–281.

Carvalho, W.A. (2002) Cyclohexane oxidation in gas phase using iron and chromium pillared clays as catalysts. *Eclética Química*, **27**, 353–365.

Chen, H.-Y. and Sachtler, W.M.H. (1998) Promoted Fe/ZSM-5 catalysts prepared by sublimation: de-NOx activity and durability in H_2O-rich stream. *Catalysis Letters*, **50**, 125–130.

Cheng, L.S. and Yang, R.T. (1995) Monolayer cuprous chloride dispersed on pillared clays for olefin-paraffin separations by π-complexation. *Adsorption*, **1**, 61–75.

Choudary, B.M., Kantam, M.L., Sateesh, M., Rao, K.K. and Santhi, P.L. (1997) Iron pillared clays – efficient catalysts for Friedel–Crafts reactions. *Applied Catalysis, A: General*, **149**, 257–264.

Clearfield, A. (1994) Pillaring studies on the some layered oxides with Ruddlesden-copper related structures. *Journal of Solid State Chemistry*, **112**, 288–294.

Duxiao, J., Nongyue, H., Yuanying, Z., Chunxiang, X., Chunwei, Y. and Zuhong, L. (2001) Catalytic growth of carbon nanotubes from the internal surface of Fe-loading mesoporous molecular sieve materials. *Materials Chemistry and Physics*, **69**, 246–251.

Guelou, E., Barrault, J., Fournier, J. and Tatibouet, J.-M. (2003) Active iron species in the catalytic wet peroxide oxidation of phenol over pillared clays containing iron. *Applied Catalysis, B: Environmental*, **44**, 1–8.

Horvath, G. and Kawazoe, K. (1983) Method for the calculation of effective pore size distribution in molecular sieve carbon. *Journal of Chemical Engineering of Japan*, **16**, 470–475.

Huerta, L., Meyer, A. and Choren, E. (2003) Synthesis, characterization and catalytic application for ethylbenzene dehydrogenation of an iron pillared clay. *Microporous and Mesoporous Materials*, **57**, 219–227.

Hutson, N.D., Hoekstra, M.J. and Yang, R.T. (1999) Control of microporosity of Al_2O_3-pillared clays: effect of pH, calcination temperature and clay cation exchange capacity. *Microporous and Mesoporous Materials*, **28**, 447–459.

Kaloidas, V., Koufopanos, C.A., Gangas, N.H. and Papanakos, N.G. (1995) Scale-up studies for the preparation of pillared layered clays at 1 kg per batch levels. *Microporous Materials*, **5**, 97.

Kantam, M.L., Choudary, B.M. and Bharathi, B. (1999) Ring opening of oxiranes catalyzed by Mn-Salen immobilized mesoporous materials. *Synthetic Communications*, **29**, 1121–1128.

Kloprogge, J.T. (1998) Synthesis of smectites and porous pillared clay catalysts: a review. *Journal of Porous Materials*, **5**, 5–41.

Kloprogge, J.T., Booy, E., Jansen, J.B.H. and Geus, J.W. (1994) The effect of thermal treatment on the properties of hydroxy-Al and hydroxy-Ga pillared montmorillonite and beidellite. *Clay Minerals*, **29**, 153–167.

Lee, H.-T. and Rhee, H.-K. (1999) Stability if Fe/ZSM-5 of NOx catalysts: Effect of iron loading and remaining Brönsted acid sites. *Catalysis Letters*, **61**, 71–76.

Long, R.Q. and Yang, R.T. (1999) Selective catalytic reduction of nitrogen oxides by ammonia over Fe^{3+}-exchanged TiO_2-pillared clay catalysts. *Journal of Catalysis*, **186**, 254–268.

Mishra, T., Parida, K.M. and Rao, S.B. (1996) Transition metal oxide pillared clay. 1. A comparative study of textural and acidic properties of Fe(III) pillared montmorillonite and pillared acid activated montmorillonite. *Journal of Colloid and Interface Science*, **183**, 176–183.

Mokaya, R. and Jones, W. (1995) The microstructure of alumina pillared acid-activated clays. *Journal of Porous Materials*, **1**, 97–110.

Molina, C.B. (2001) Síntesis y caracterización de arcillas pilareadas y su aplicación con catalizadores en la reducción selectiva de NOx. PhD thesis, Universidad de Castilla La Mancha, Ciudad Real, España.

Palinko, I., Lazar, K., Hannus, I. and Kirisci, I. (1996) Step toward nanoscale Fe moieties: intercalation of simple and Keggin-type iron-containing ions in-between the layers of Na-montmorillonite. *Journal of Physics and Chemistry of*

Solids, **57**, 1067–1072.

Rightor, E.G., Tzou, M.S. and Pinnavaia, T.J. (1991) Iron oxide pillared clay with large gallery height: synthesis and properties as a Fischer-Tropsch catalyst. *Journal of Catalysis*, **130**, 29–40.

Shabatai, J., Rosell, M. and Torkarz, M. (1984) Cross-linked smectites III. Synthesis and properties of hydroxyl-aluminum hectorites and fluorhectorites. *Clays and Clay Minerals*, **35**, 99–107.

Sharpe, A.G. (1993) *Química Inorgánica*. Reverté S.A., Barcelona, Spain.

Sing, K.S.W., Everett, D.H., Haul, R.A.W., Moscou, L., Pierotti, R.A., Rouquerol, J. and Siemieniewska, T. (1985) Reporting physisorption data for gas/solid systems with special reference to the determination of surface area and porosity (Recommendations 1984). *Pure and Applied Chemistry*, **57**, 603–619.

Sprung, R., Davis, M.E., Kauffman, J.S. and Dybowski, C. (1990) Pillaring of magadiite with silicate species. *Industrial & Engineering Chemistry Research*, **29**, 213–220.

Tzou, M.S. and Pinnavaia, T.J. (1983) Chromia pillared clays. *Catalysis Today*, **2**, 243–259.

Valverde, J.L., Sanchez, P., Dorado, F., Molina, C.B. and Romero, A. (2002) Influence of the synthesis conditions on the preparation of titanium-pillared clays using hydrolyzed titanium ethoxide as the pillaring agent. *Microporous and Mesoporous Materials*, **54**, 155–165.

Valverde, J.L., Sanchez, P., Dorado, F., Asencio, I. and Romero, A. (2003) Preparation and characterization of Ti-pillared clays using Ti alkoxides. Influence of the synthesis parameters. *Clays and Clay Minerals*, **51**, 41–51.

Van Olphen, H. (1963) *An Introduction to Clay Colloid Chemistry*, 2nd edition. Wiley, New York.

Webb, P.A. and Orr, C. (1997) *Analytical Methods in Fine Particle Technology*, 1st edition. Micromeritics Instrument Corp. Norcross, Georgia, USA.

Yamanaka, S., Nishihara, T., Hattori, M. and Suzuki, Y. (1987) Preparation and properties of titania pillared clay. *Materials Chemistry and Physics*, **17**, 87–101.

Yang, R.T., Chen, J.P., Kikkinides, E.S., Cheng, L.S. and Cichanowicz, J.E. (1992) Pillared clays as superior catalysts for selective catalytic reduction of nitric oxide with ammonia. *Industrial & Engineering Chemistry Research*, **31**, 1440–1445.

Zurita, M.J., Vitale, G., De Goldwasser, M.R., Rojas, D. and García, J.J. (1996) Fe-pillared clays: A combination of zeolite shape selectivity and iron activity in the CO hydrogenation reaction. *Journal of Molecular Catalysis*, **107**, 175–183.

(*Received 21 October 2004; revised 20 May 2005; Ms. 973; A.E. James E. Amonette*)